Chapter 19
New Criteria for Brine Discharge Outfalls from Desalination Plants

Raed Bashitialshaaer, Kenneth M. Persson and Magnus Larson

Abstract An efficient method for increasing the dilution rate of brine water discharged into the sea is an inclined negatively buoyant jet from a single port or a multi-diffuser system. Such jets typically arise when brine is discharged from desalination plants. Two small-scale experimental studies were conducted to investigate the behaviour of a dense jet discharged into lighter ambient water. The first experiment concerned the importance of the initial angle of inclined dense jets, where the slope of the flow increased for the maximum levels as a function of this angle. An angle of 60° produced better results than 30° or 45°. An empirical predictive equation was developed based on five geometric quantities to be considered in the design of plants. The second experiment studied the near and intermediate fields of negatively buoyant jets. Dilution in the flow direction was increased by about 10 and 40 % with bottom slope, and bottom slope together with a 30° jet inclination, respectively. An over 16 % bottom slope experiment and more field work in the future are needed to compare with this result. It was found that an inclination of 30° with a 16 % bottom slope were optimal for the design of brine discharge outfall.

19.1 Introduction

In desalination, high-salinity brine is produced that needs to be discharged into a receiving water body with a minimum of environmental impact. Nowadays, brine discharge from desalination plants is the concern of all countries producing fresh water from desalination with different technologies.

R. Bashitialshaaer (✉) · K.M. Persson · M. Larson
Department of Water Resources Engineering, Lund University, Lund, Sweden
e-mail: ralshaaer@yahoo.com

K.M. Persson
e-mail: Kenneth_m.perrson@tvrl.lth.se

M. Larson
e-mail: Magnus.Larson@tvrl.lth.se

The brine is typically discharged as a turbulent jet (Turner 1966) with an initial density that is significantly higher (salinity 4–5 %) than the density of the receiving water (ambient e.g. seawater). Thus, a rapid mixing of the discharged brine is desirable to ensure minimum impact, which requires detailed knowledge of the jet development. Since the density of the jet is greater than the density of the receiving water, the jet is negatively buoyant and it will impinge on the bottom some distance from the discharge point depending on the initial momentum, buoyancy, and angle of the discharge, as well as the bathymetric conditions. After the jet encounters the bottom it will spread out as a gravity current with a low mixing rate, making it important to achieve the largest possible dilution rate when the jet moves through the water column.

In an early study, Zeitoun et al. (1972) investigated an inclined jet discharge, focusing on an initial jet angle of 60° because of the relatively high dilution rates achieved for this angle. Roberts and Toms (1987) and Roberts et al. (1997) also focused on the 60° discharge configuration, where both the trajectory and dilution rate were measured. Cipollina et al. (2005) extended the work performed in previous studies on negatively buoyant jets discharged into calm ambient by investigating flows at different discharge angles, namely 30°, 45°, and 60°, and for three densities 1055, 1095 and 1179 kg/m^3. Kikkert et al. (2007) developed an analytical solution to predict the behavior of inclined negatively buoyant jets, and reasonable agreement was obtained with measurements for initial discharge angles ranging from 0° to 75° and initial densimetric Froude numbers from 14 to 99. Submerged negatively buoyant jets discharged over a flat or sloping bottom, covering the entire range of angles from 0° to 90°, were investigated by Jirka (2006) in order to improve design configurations for desalination brine discharges into coastal waters. Jet experiment measurement can be affected with possible related errors depending on the type and amount of dye, the illumination level, and the sensitivity of the recording method (Jirka 2008).

Christodoulou and Papakonstantis (2010) studied negatively buoyant jets with discharge angles between 30° and 85°. By fitting empirical equations to relevant experimental data they estimated that the trajectory of the upper boundary and the jet axis (centerline) could be approximated in non-dimensional form by a 2nd degree polynomial (parabola). Mixing and re-entrainment are both important in negatively buoyant jets. These phenomena have been experimentally studied and discussed by (Ferrari and Querzoli 2010). They found that re-entrainment tends to appear if the angle exceeds 75° with respect to the horizontal, and the onset occurs for lower angles as the Froude number increases. The re-entrainment makes the jet trajectory bend on itself, causing a reduction of both the maximum height and the distance to the location where entrainment of external fluid reaches the jet axis (Ferrari and Querzoli 2010). Papakonstantis et al. (2011) studied six different discharge angles for negatively buoyant jets from 45° to 90° to the horizontal. In their experiment they used a large-size tank and also measured the horizontal distance from the source to the upper (outer) jet boundary at the source elevation.

It was possible to investigate the effects of turbulent energy on the initial development and large scale instabilities of a round jet by placing grids at the

nozzle outlet to alter the jet initial conditions because the grids causes small scale injection of turbulent energy (Burattini et al. 2004). The jet lateral spreading and consequent dilution at the bottom is of considerable practical importance in assessing the environmental impact of the effluent on the receiving water at the discharge point (Christodoulou 1991). The behavior of a laterally confined 2-D density current has been considered in past but the numbers on a 3-D system are very limited (Ellison and Turner 1959; Benjamin 1968; Simpson 1987). Hauenstein and Dracos (1984) proposed an integral model based on similarity assumptions, which was supported by their laboratory experimental data of the radial spreading of a dense current inflow into a quiescent ambient.

Previous studies mainly focused on the separate analysis of near-field and intermediate-field properties of buoyant jets and plumes. Some hypotheses on how to connect the two different zones have also been proposed. Turner and Abraham were the first to analyze this kind of problem of a vertical negatively buoyant jet (Turner 1966; Abraham 1967). The dense layer spreads in all directions at a rate proportional to the entrainment coefficient (Alavian 1986). His result was obtained by flowing salt solution (4 g/l) on a sloping surface in a tank of freshwater and his experimental result was based on three different inflow buoyancy fluxes on three angles of incline of 5°, 10°, and 15° (Alavian 1986). Akiyama and Stefan (1984) developed an expression for the depth at the plunge point as a function of inflow internal Froude number, mixing rate, bed slope, and total bed friction. Christodoulou (1991) described theoretically the main factors affecting near-, intermediate-, and far-field properties, suggesting appropriate length scales for each zone. Suresh et al. (2008) investigated the lateral spreading of plane buoyant jets and how they

Table 19.1 Dispersion tanks with different sizes used in earlier experiments (excerpted from Bashitialshaaer and Persson 2012)

Previous study	Cross-section (m)	Depth (m)
Turner (1966)	0.45 × 0.45	1.40
Demetriou (1978)	1.20 × 1.20	1.55
Alavian (1986)	3.0 × 1.50	1.50
Lindberg (1994)	3.64 × 0.405	0.508
Roberts et al. (1997)	6.1 × 0.91	0.61
Zhang and Baddour (1998)	1.0 × 1.0	1.0
Pantzlaff and Lueptow (1999)	D = 0.295	0.89
Bloomfield and Kerr (2000)	0.40 × 0.40	0.70
Cipollina et al. (2005)	1.50 × 0.45	0.60
Jirka (1996, 2004, 2006)	CORMIX, CorJet	
Kikkert et al. (2007)	6.22 × 1.54	1.08
Papanicolaou and Kokkalis (2008)	0.80 × 0.80	0.94
Shao and Law (2010)	2.85 × 0.85	1.0
This study	1.50 × 0.60	0.60
	2.0 × 0.50	0.60

depend on the Reynolds number, suggesting and demonstrating that a reduction of the spreading occurs with an increase in the Reynolds number. Table 19.1 is the summary of different sizes that have been used for laboratory mixing tank dimensions (L × W × H) as found in literature.

19.2 Objectives and Procedures

The water intake to most of the world's desalination plants is located close to where the brine is discharged. Some chemicals and other parameters have to be considered as a function of the brine discharge from desalination plants to assist people from an environmental and economic perspective, e.g. fishing problems could increase in the future. More objectives were added to this study in order to find the relationships between an increase in desalination plant production and salinity increase in the recipient. Thus, the main objective of this study is to find out the most efficient way to reduce the impact of brine discharge from desalination plants by improving the mixing conditions in the discharged jet. Therefore, it was decided to perform small-scale laboratory experiments. Two sets of experiments were conducted for negatively buoyant jet, each with a total of 72 runs in order to:

- Understand jet behaviour when brine is discharged into a stagnant ambient and to find the maximum elevated level of the jet.
- Find the effect of the initial jet angle on the mixing between a denser fluid comprised of a sodium chloride solution and tap water.
- Evaluate the importance of bottom slope with and without inclination and the effect of lateral spreading and centreline concentration.
- Possibility to compare collected data with simulation results using hydraulic modelling software, e.g. CORMIX.

19.2.1 Laboratory Experiments

19.2.1.1 Experimental Setup

The experiments on inclined negatively buoyant jets were carried out in the laboratory of Water Resources Engineering at Lund University. The apparatus and major equipment used in the experiments included water tanks, a flow meter, a digital frequency recorder, a digital conductivity meter, pump to fill and empty the tanks, pipes, valves, nozzles and nozzle support, salt, and dye (Fig. 19.1). Several different tanks were used in the experiment: (1) a small tank to mix tap water with salt and a coloring dye for generating an easy to visualize negatively buoyant jet of saline water; (2) two elevated small tanks used to create the hydraulic head for generating the jet; and (3) a large tank made with glass walls filled with tap water
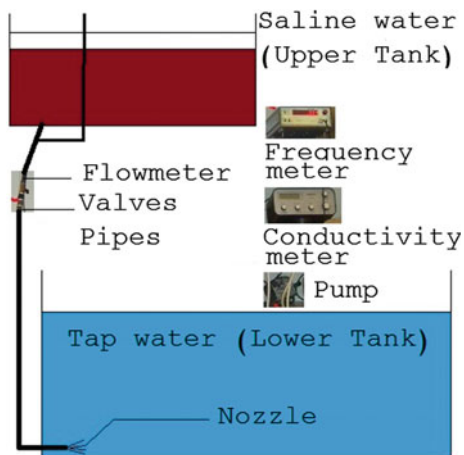
Fig. 19.1 Experimental setup and major components used (Bashitialshaaer et al. 2013)

(fresh water) where the jet was introduced through a nozzle. The small tanks were made of plastic and their volumes were 45, 70, and 90 L, whereas the maximum volume of the large tank was 540 L with bottom area dimensions of 150 cm × 60 cm and a height of 60 cm. Two of the smaller tanks were placed at a higher elevation compared to the large tank to create the necessary hydraulic head for driving the jet. These two tanks were connected by a pipe and together they had a sufficiently large capacity (i.e., surface area) to keep the water level approximately constant in the two tanks during the experiment to ensure a constant flow. The difference in elevation between the water levels of the upper tanks and the lower tank was about 100 cm. The colored saltwater from the upper tanks was discharged through a plastic, transparent pipe directly connected to the jet nozzle, which was fixed at the bottom of the large water tank. Between the elevated tanks and the nozzle there was a valve to control the flow to the nozzle. A flow meter was installed in the pipe between the valve and the outlet from the upper tanks in order to record the initial jet flow. This meter was connected to a digital frequency recorder, from which the readings were converted into flow rates based on a previously derived calibration relationship.

19.2.1.2 Experimental Procedure and Data Collected

Before starting an experimental case, it was crucial to empty the pipe leading from the upper tanks of air. This was done by attaching a special pipe to the flow meter and discharging tap water through this pipe, forcing out the air from the system. After each experimental case a submersible water pump was used to completely empty the large tank, so that each case started with water that was not contaminated by salt. With the capacity of the pump, it took about 12 min to empty the tank. Also,

the whole system was regularly washed to avoid accumulation of salt, which would disturb the experiment. Potassium permanganate ($KMnO_4$) was used to color the saline water and make the jet visible during the experiment. About 100 mg/L of dye gives the transparent water a distinct purple color. The use of a colored jet facilitated the observation of the jet trajectory and the mixing behavior in the larger water tank. The results of jar tests for different ($KMnO_4$) concentrations showed that at a concentration of 0.3 mg/L the water is still colored, whereas at a concentration of 0.2 mg/L no color was visible to the eye.

During a specific case, the jet was discharged for a sufficiently long time to allow steady-state conditions to develop, but short enough to avoid unwanted feedback from saline water accumulating in the tank (the duration of an experimental case was normally about 3–5 min). The jet trajectory and its geometric properties were determined by tracing the observed trajectory on the glass wall of the flume. The outer edges of the jet were traced and the center line was determined as the average between these two lines. In order to minimize the influence of the subjective element in tracing the jet, a number of different people were involved in this procedure to ensure that the results were consistent, in agreement, and reproducible. Also, the experimental cases were recorded with a video camera and subsequently viewed. Three cases did not produce satisfactory data due to malfunctioning, and here the results from 69 cases are reported.

19.2.1.3 Inclined Jet Experiment

Fine, pure sodium chloride was used with tap water to produce the saline water in the jet. The necessary water quantity was measured in a bucket and the mass of salt was measured using a balance to obtain the correct salt concentration. A conductivity meter was employed to measure the conductivity for the three different initial concentrations investigated. The density measurements for these concentrations yielded 1011, 1024 and 1035 kg/m^3 for 2, 4 and 6 %, (20, 40, and 60 g/L), respectively. The temperature of the tap water used in this experiment was in the range 20–22 °C for all cases, implying a density of about 995.7 kg/m^3. Each of the densities was the average of five different measurements based on the weight method. Differences in density were observed between the salt water used in this study and natural seawater. The chemical composition of seawater is different from the sodium chloride solutions used here, although the density varies only slightly in seawater compared to the pure sodium chloride solutions. The parameters of interest were:

- Diameter of nozzle, d_o (4.8; 3.3; 2.3, 1.5 mm)
- Initial jet angle, θ to the horizontal line (30°, 45°, 60°)
- Salinity of brine discharge S (2; 4; 6 %)

19.2.1.4 Near and Intermediate Zone Experiment

The apparatus and major materials used in the experiment in the laboratory were water tanks, flow-meter, digital frequency-meter, digital conductivity meter, pump, pipes, valves, nozzles and nozzle support, salt and dye (see Fig. 19.1). Preliminary measurements were conducted after calibrating the apparatus in order to obtain reference data and to check if our measurement tools (i.e. flow meter, conductivity meter) were reliable and coherent with literature data. These measurements included flows, water salinity, density, and conductivity, basic information about water density and conductivity variation as a function of salinity at a constant room temperature of 20 ± 1 °C. Each experimental run was characterized by a set of parameters, and the first step of each run was used to find the proper combination of parameter values. The parameters of interest were:

- Diameter of nozzle, d_o (4.8; 3.3; 2.3 mm)
- Initial jet angle, θ to the horizontal line (0; 30°)
- Bottom slope S_b (0; 16 %), the tank tilting
- Salinity of brine discharge S (4; 6; 8 %)

19.3 Theoretical Considerations

19.3.1 Inclined Negatively Buoyant Jets

An inclined negatively buoyant jet discharged upwards at an angle towards the horizontal (Fig. 19.2) represents the typical case of a brine jet discharged into receiving water. The jet describes a trajectory that reaches a maximum level, after which the jet changes its upward movement and plunges towards the bottom. Since the jet is negatively buoyant, the initial vertical momentum flux driving the flow upwards is continuously reduced by the buoyancy forces until this flux becomes zero at the maximum level and the jet turns downwards.

Knowledge of the shape of the jet trajectory is important in the design of brine discharge. Major variables that previously were employed to describe the jet trajectory (with respect to the location of the jet origin based on a x-y coordinate system) are: the maximum level of the jet centerline Y and its horizontal distance X_y, the maximum level of jet flow edge Y_m, and its horizontal distance X_{ym}, X_i is the jet centerline impact point distance and X_e the maximum horizontal distance to the jet flow edge point, where the jet returns to the discharge level (Fig. 19.2). In general, the location of the jet edge may be defined as the maximum jet height boundary at any particular location.

The jet is discharged at a flow rate Q_o through a round nozzle with a diameter d_o, yielding an initial velocity of u_o, and at an angle θ to the horizontal plane. The initial density of the jet is ρ_o and the density of the receiving water (ambient) ρ_a,
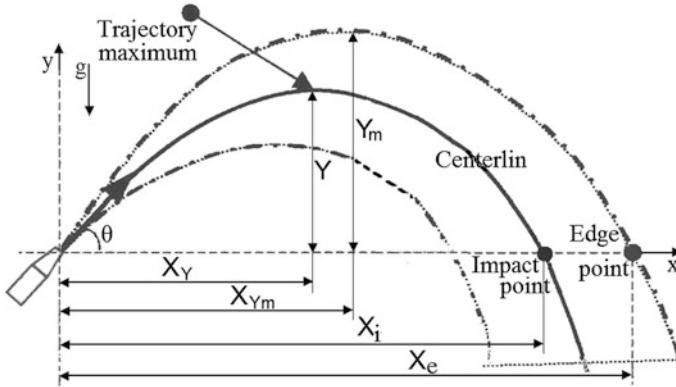
Fig. 19.2 Definition sketch for inclined jet parameters (after Cipollina et al. 2005)

where $(\rho_o > \rho_a)$, giving an initial excess density in the jet of $\Delta\rho = (\rho_o - \rho_a) \ll \rho_a$ (the Boussinesq approximation). Similar flow problems were previously analyzed through dimensional analysis (e.g., Turner 1966; Roberts and Toms 1987; Pincince and List 1973; Cipollina et al. 2005; Fischer et al. 1979). Most previous studies assumed that the Boussinesq approximation is valid and that the flow is fully turbulent. Thus, the initial jet properties can be characterized by the volume flux Q_o, the kinematic momentum flux M_o, and the buoyancy flux B_o, as defined by Fischer et al. (1979), together with the initial jet angle θ (the subscript o denotes conditions at the nozzle). The leading variables in the dimensional analysis may be written for a round jet with uniform velocity distribution at the exit:

$$Q_o = \frac{\pi d_o^2}{4} u_o, \quad M_o = \frac{\pi d_o^2}{4} u_0^2, \quad B_o = g\frac{\rho_o - \rho_a}{\rho_a} Q_o = g'Q_o \qquad (19.1)$$

where g is acceleration due to gravity; and $g' = g(\rho_o - \rho_a)/\rho_a$ is the modified acceleration due to gravity. A dimensional analysis involving Q_o, M_o, and B_o yields two length scales that may be used to normalize the above-mentioned geometric quantities and to develop empirically based predictive relationships (Fischer et al. 1979):

$$l_M = \frac{M_o^{3/4}}{B_o^{1/2}} \quad \text{and} \quad l_Q = \frac{Q_o}{M_o^{1/2}} \qquad (19.2)$$

By using the bulk quantities Q_o, M_o, and B_o, the nozzle shape and the initial velocity distribution is implicitly taken into account. For a uniform velocity distribution, $l_Q = \sqrt{A_o}$ and if the nozzle is circular $l_Q = d_0\sqrt{\frac{\pi}{4}}$. In the two sets of experiments a densimetric Froude number F, is defined by $(u_0/\sqrt{g'd_0})$. More details and equations can be found in (Bashitialshaaer et al. 2012).

19.3.2 Near and Intermediate

Brine discharge from a desalination plant is an example of denser fluid discharge to a stagnant ambient from a single port or a multiport at angle θ, with bottom slope S_b. This flow may be conceptually divided into three connected regions, the near-field, the intermediate field and the far-field. The near-field is the initial flow or development region (named the potential core for a top-hat exit profile); it is usually found within ($0 \leq x/d_0 \leq 6$). The far-field is the fully-developed region where the thin shear layer approximations can be shown (with appropriate scaling); jet flows generally become self-similar beyond ($x/d_0 \geq 25$) (Christopher and Andrew 2007). The intermediate-field, or transition region, lies between the near- and far-fields of the jet. Method of understanding mixing in intermediate-field or transition was well defined qualitatively by flow visualization e.g. (Dimotakis 2000; Dimotakis et al. 1983). In the intermediate region of a round jet there was only Reynolds dependence of shear stress distributions as shown in (Matsuda and Sakakibara 2005). They used method of a stereo particle image velocity (PIV) system. The mean and fluctuating velocity curves were plotted for Re = 1500; 3000; 5000. The lateral spreading of the jet is shown in Fig. 19.3 in two dimensions x-axis and y-axis, in which b(x) was measured at three locations b_1, b_2 and b_3 at horizontal distances X_1, X_2 and X_3 for 20, 40 and 60 cm respectively (Bashitialshaaer and Persson 2012).

  Considering a negatively buoyant jet, the dilution at the impact point S_d in the near-field from a single port into a stagnant ambient comes with some assumptions. For the jet to retain its identity, the discharge angle should not be too small to avoid attachment to the bottom or too large to avoid falling on itself (Christodoulou 1991). The terminal minimum dilution at the impact point can be written in terms of the main variables as:
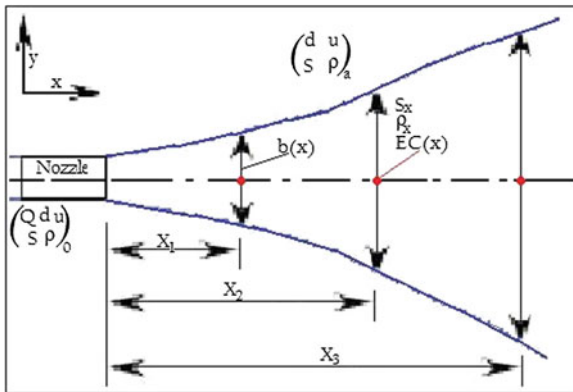
$$S_d = f(Q_0, M_0, B_0, \vartheta) \tag{19.3}$$

Fig. 19.3 Plan view of lateral jet spreading and the measurements locations (Bashitialshaaer and Persson 2012)

The effect of the initial discharge is normally small and negligible, after a simple dimensional analysis the initial dilution is given by $S_d = f_1(\theta, F)$, where F is a Froude densimetric number as defined before. A Froude number of 10 or larger simplifies the above equation to $(F/S_d) = c(\theta)$, where the constant c is a function of inclined angle θ. Previously this constant was determined experimentally by many people, e.g. (Roberts and Toms 1987) for a 60° inclined angle as a value of c = 1.03; for the same angle (Zeitoun et al. 1970) presented an earlier estimation for c of about 1.12. In the description of the intermediate field lateral spreading of the dense plume along a mildly sloping bottom, one should take into account that at small slopes, the entrainment is small and negligible (Ellison and Turner 1959; Alavian 1986; Britter and Linden 1980). Therefore, the width of the plume should depend mainly on the buoyancy flux, the bottom roughness (drag coefficient C_d) and the geometrical characteristics of the problem (Christodoulou 1991). Thus, the lateral spreading width b downstream a distance x can be written as:

$$b = f(x, b_0, B_0, S_b, C_d, g) \tag{19.4}$$

From dimensional analysis Eq. (19.4) can be written as:

$$\frac{b}{b_0} = f_1\left(\frac{x}{b_0}, \frac{B_0}{g^{3/2}b_0^{5/2}}, S_b, C_d\right) \tag{19.5}$$

Alavian (1986) suggested that the terminal to initial width ratio b_n/b_0 is essentially independent of the slope for $5° \leq S_b \leq 15°$, although the rate of approach to the normal state is faster for smaller slopes. From the above statement the determination of the terminal width b_n for relatively small slopes (less than about 15°), the explicit inclusion of S_b in, Eq. (19.5) can be omitted:

$$\frac{b_n}{b_0} \approx f_2\left(\frac{B_0}{g^{3/2}b_0^{5/2}}, C_d\right) \tag{19.6}$$

A power law form for Eq. (19.6) yields:

$$\frac{b_n}{b_0} = K\left(\frac{B_0}{g^{3/2}b_0^{5/2}}\right)^a \tag{19.7}$$

where $K = k(C_d)$. Equation (19.7) has been tested against limited experimental data in (Alavian, 1986) and numerical results in Tsihrintzisand and Alavian (1986). They referred to a distance $x = 100b_0$, where the spreading width had not yet strictly reached a constant value, apparently due to the low drag coefficient employed. The value of the exponent was estimated in Christodoulou (1991), as a = 0.183, while k exhibits an increasing trend with decreasing C_d.

19.3.3 Model Assumptions

The modeling assumption of the jet and plume evolution was essentially divided into two sub-models, that is, the near field and the intermediate field. The near field is the proximity of the nozzle, where jet and plume development is driven by the initial conditions; i.e. the initial momentum flux, volume flux, and buoyancy flux, and there is no interaction with the bottom. In the intermediate field, the buoyant jet essentially becomes a plume (gravity current) and it is interacting with the bottom. The main forces to be considered are bottom drag force and bottom slope effects. The "intermediate field" begins when the buoyant jet reaches the bottom. To develop a simple model describing the situation in the proximity of the discharge nozzle, some assumptions were made (see Bashitialshaaer and Persson 2012).

19.4 Results and Discussion

19.4.1 General Development

A very strong correlation between Y_m and Y was found, lending some confidence to the accuracy of the measurements. The least-square fitted line through the origin yields a slope of about 1.25, implying that Y_m on average is about 25 % larger than Y. Similarly, between X_y and X_{ym}, a coefficient value of about 1.20 was obtained, which is somewhat lower than that in the relationship between Y and Y_m. Furthermore, the horizontal distance to the edge point of the jet (X_e) showed a rather good correlation with X_{ym} (or X_y), approximately 1.65. Thus, if the vertical and horizontal distance to the maximum centerline level (or, alternatively, the maximum jet edge level) can be predicted, other geometric quantities can be calculated from the following regression relationships:

$$\left.\begin{array}{l} Y_m = 1.25\,Y \\ X_{ym} = 1.20\,X_y \\ X_e = 1.65\,X_{ym} \end{array}\right\} \tag{19.8}$$

The relationship between the maximum levels and their horizontal distances displayed more scatter (Fig. 19.4) and included a dependence on the initial jet angle. However, a general equation of linear type could be fitted through the data points with reasonable accuracy ($Xy = k_\theta Y$), where k_θ is an empirical coefficient that takes on the value 2.3, 1.5, and 1.0 for the initial jet angle 30°, 45°, and 60°, respectively. If a simple ballistics model was employed to describe the jet trajectory (i.e., constant g'), the ratio between X_y and Y would be given by $2/(\tan \vartheta)$, which yields the following slopes for the lines: 3.5, 2.0, and 1.2. A similar equation could be developed for X_{ym} and Y_m.
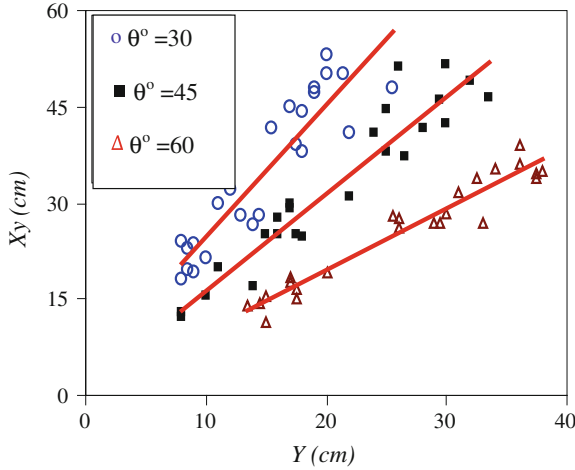
Fig. 19.4 Maximum jet centerline level versus its horizontal distance with respect to initial jet angle

19.4.2 Developing Relationships

Equation $(Y/l_M) = K$ indicates that there is a linear relationship between the normalized quantities that describe the jet trajectory and F. However, this is based on the assumption that $l_m \gg l_Q$, otherwise this equation $(Y/l_M) = f(l_m/l_Q)$ should be employed, developing this relationship by introducing the definition of the length scales yields:

$$\frac{Y}{d_0} = k * F * \Psi(F) \tag{19.9}$$

where Ψ = function and Y is used as an example of a geometric jet quantity. If F is small $\Psi(F) \rightarrow 1$, whereas for large F values $Y \rightarrow \infty$. The data indicates a relationship, where $Y/d_0 \propto F^n$, with $n < 1$. Based on the theoretical constraints and the empirical observations, the following equation was proposed to describe Y/d_o as a function of F over the entire range of experimental data:

$$\frac{Y}{d_0} = \frac{k * F}{(1 + \alpha F)^m} \tag{19.10}$$

where α and m are empirical coefficients obtained from fitting against data. Equation 19.10 can be approximated with a straight line in accordance with relation $(Y/d_0) = (k * F)$ for small values on α F. where $k = K(\pi/4)^{1/4}$. Similar equations may be developed for the other geometric jet quantities Y_m, X_y, X_{ym}, and X_e, but with different values of the coefficient k. Figure 19.5 shows an example of
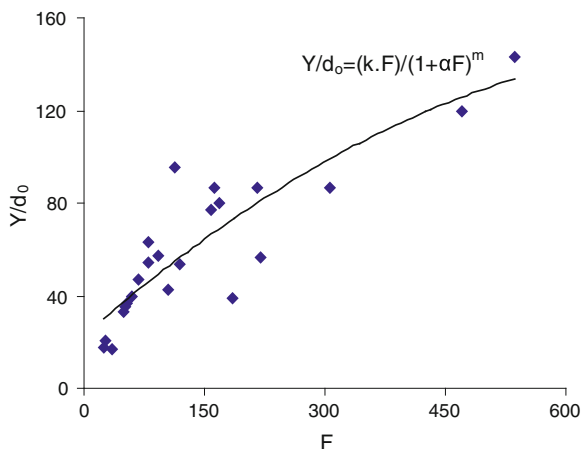
Fig. 19.5 Normalized maximum jet centerline level as a function of (F) for an initial jet angle of 30°

least-square fitting of Eq. 19.10 against the data for the maximum jet centerline level (Y) and an initial jet angle of 30°, where the optimum values of k, α, and m were determined as 1.35, 0.008, and 0.8, respectively.

19.4.3 Bottom Slope Effects

The electrical conductivity ratio and the lateral spreading were compared with and without bottom slope at three horizontal distances 20, 40 and 60 cm, that results in small variations between flow on a horizontal bed and a slope. The correlations between the two cases are in the range 86–89 %, which means the sloping bottom does not affect the flow regime. For the lateral spreading, it was also shown that the correlation is 88–91 %, much better than for the electrical conductivity.

Normalized lateral spreading (b/d_0) and thickness of the dense layer (z/d_0) are compared for four cases at horizontal distances 20, 40 and 60 cm along the x-axis with respect to the inclined angle (θ) and bottom slope (S_b). Different comparisons were made between measured parameters to see the effects of the initial angle and bottom slope. First we compared the normalized lateral spreading at three different positions, inclined angle ($\theta = 0°$) and bottom slope ($Sb = 0°$) versus ($\theta = 30$, $Sb = 0$); ($\theta = 0$, $Sb = 16$); ($\theta = 30$, $Sb = 16$). For the lateral spreading the trend line showed good correlation above 80 %, except for one of them.

Figure 19.6 presents the experimental results for the concentration (in percentage) that were measured at three distances along the flow, comparing with and without bottom slope for densimetric Froude numbers smaller and larger than 40. The concentration along the flow was improved by about 10 % with the bottom
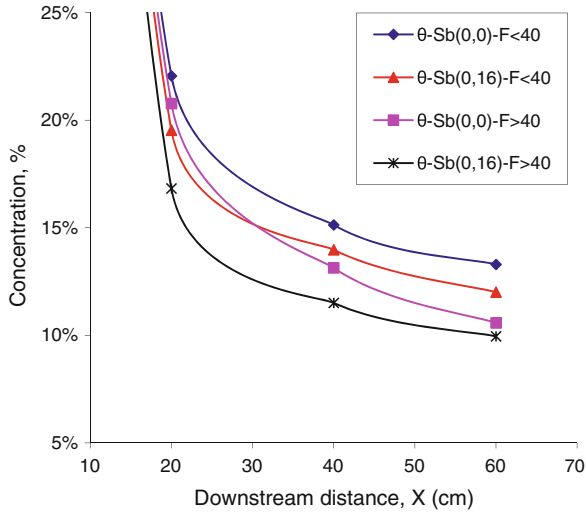
Fig. 19.6 Concentration in percentage along the flow with and without bottom slope
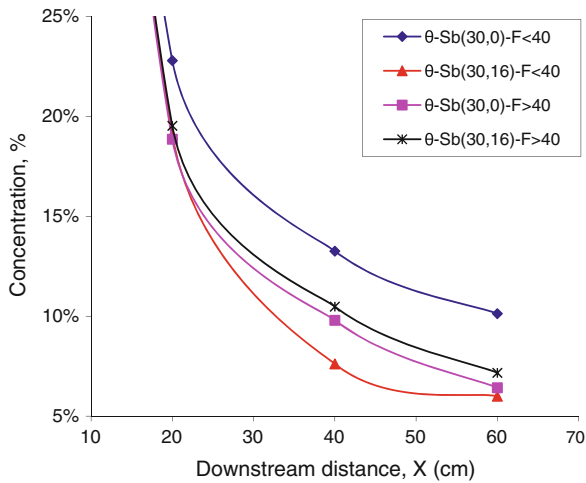

Fig. 19.7 Concentration in percentage along the flow with and without bottom slope (with 30° inclination)

slope for Froude number smaller than 40 which can be used for real discharge cases. Thus, this type of improvement can be used for brine discharge outlet to the recipients to minimize the concentration and let it dilute faster and go farther. Another comparison is presented in Fig. 19.7, also with and without bottom slope,

but this time including jet inclination angle of 30°. It also shows improvement in the concentration reduction of about 40 % with bottom slope and inclination for Froude numbers smaller than 40, but small differences for Froude numbers larger than 40.

19.5 Conclusions

The purpose of this study was originally to be able to determine the properties of different jet discharges with regard to bottom slope in the recipient and varying initial jet inclination angle. Desalination brine is the practical case to consider when studying environmental impact and assessment in connection with new projects. In reality, most of the recipients, e.g., marginal seas and oceans, naturally have a bottom slope, and it varies from one place to another. Two sets of laboratory experiments were conducted to investigate the behavior of negatively buoyant jets discharged at an angle to the horizontal into a quiescent body of water that may have a sloping bottom.

Several of the geometric jet quantities showed strong correlation and regression relationships could be developed where one quantity could be predicted from another. If maximum levels were correlated with the corresponding horizontal distances, the angle must be taken into account when developing predictive relationships in real life projects. It is believed that the empirical relationships developed in this study have a potential for use in practical design where the trajectory of brine jets needs to be estimated. Equations were proposed to relate levels and horizontal distances to each other.

Based on the findings in this study in the near- and intermediate regions the flow geometry depends on the angle of inclination and the rate of supply of the dense fluid. After an initial spreading, the flow geometry becomes relatively constant with the horizontal distance down the slope. For a given buoyancy flux, the normal layer width seems to weakly depend on slope. Lowering of the concentration (through mixing) was improved with the bottom slope by 10 % compared to the horizontal bottoms and improved by about 40 % with bottom slope together with an inclination of 30°. A suggestion in practical applications concerning desalination brines and similar discharge of heavy wastes is to have an inclination and a bottom slope together. This study is based on limited experiments for only 16 % bottom slope and 30° inclination; thus, further experimental work is needed.

References

Abraham, G. (1967). Jets with negative buoyancy in homogeneous fluids. *Journal of Hydraulic Research, 5*, 236–248.

Akiyama, J., & Stefan, H. G. (1984). Plunging flow into a reservoir: Theory. *Journal of Hydraulic Engineering, ASCE, 110*(4), 484–499.

Alavian, V. (1986). Behavior of density currents on an incline. *Journal of Fluid and Mechanics, ASCE, 112*(1), 27–42.

Bashitialshaaer, R., & Persson, K. M. (2012). Near and intermediate field Evolution of a negatively buoyant jet. *Journal of Basic and Applied Sciences, 8*(2), 513–527.

Bashitialshaaer, R., Larson, M., & Persson, K. M. (2012). An experimental investigation on inclined negatively buoyant jets. *Water: Advances in Water Desalination, 4*(3), 720–738. doi:10.3390/w4030720.

Bashitialshaaer, R., Larson, M., & Persson, K. M. (2013). An Experimental study to improve the design of brine discharge from desalination plants. *American Journal of Environmental Protection, 2*(6), 176–182.

Benjamin, T. B. (1968). Gravity currents and related phnonmena. *Journal of Fluid Mechanics, 31* (2), 209–248.

Bloomfield, L.J., & Kerr, R.C. (2000). A theoretical model of a turbulent fountain, *Journal of Fluid Mechanics*, *424*, 197–216.

Britter, R. E., & Linden, P. E. (1980). The motion of the front of a gravity current travelling down an incline. *Journal of Fluid and Mechanics, 99*(3), 531–543.

Burattini, P., Antonia, R. A., Rajagopalan, S., & Stephens, M. (2004). Effect of initial conditions on the near-field development of a round jet. *Experiments in Fluids, 37*, 56–64.

Christodoulou, G. C. (1991). Dilution of dense effluents on a sloping bottom. *Journal of Hydraulic Research, 29*(3), 329–339.

Christodoulou, G. C., & Papakonstantis, I. G. (2010). Simplified estimates of trajectory of inclined negatively buoyant jets. In *Environmental hydraulics* (pp. 165–170). London, UK: Taylor & Francis.

Christopher, G. B., & Andrew, P. A. (2007). *Review of experimental and computational studies of flow from the round jet.* Queen's University, Kingston, Ontario, Canada, INTERNAL REPORT No. 1, CEFDL., 2007/01.

Cipollina, A., Brucato, A., Grisafi, F., & Nicosia, S. (2005). Bench scale investigation of inclined dense jets. *Journal of Hydraulic Engineering Division of the American Society of Civil Engineers, 131*, 1017–1022.

Dimotakis, P. E. (2000). The mixing transition in turbulent flows. *Journal of Fluid Mechanics, 409*, 69–98.

Dimotakis, P. E., Miake-Lye, R. C., & Papantoniou, D. A. (1983). Structure and dynamics of round turbulent jets. *Physics of Fluids, 26*, 3185–3192.

Demetriou, J.D. (1978). Turbulent diffusion of vertical water jets with negative buoyancy (In Greek), Ph.D. Thesis, Greece: National Technical University of Athens.

Ellison, T. H., & Turner, J. S. (1959). Turbulent entrainment in stratified flows. *Journal of Fluid Mechanics, 9*, 423–448.

Ferrari, S., & Querzoli, G. (2010). Mixing and re-entrainment in a negatively buoyant jet. *Journal of Hydraulic Research, 48*, 632–640.

Fischer, H. B., List, E. J., Koh, R. C. Y., Imberger, J., & Brooks, N. H. (1979). *Mixing in inland and coastal waters*. New York, NY, USA: Academic Press.

Hauenstein, W., & Dracos, T. H. (1984). Investigation of plume density currents generated by inflows in lakes. *Journal of Hydraulic Research, 22*(3), 157–179.

Jirka, G.H., Doneker, R.L., & Steven, W.H. (1996). *User's manual for CORMIX: A hydrodynamic mixing zone model and decision support system for pollutant discharges into surface waters*. DeFrees Hydraulics Laboratory School of Civil and Environmental Engineering, Cornell University

Jirka, G.H. (2004). Integral model for turbulent buoyant jets in unbounded stratified flows, Part 1: The single round jet. *Environmental Fluid Mechanics*, *4*, 1–56.

Jirka, G. H. (2006). Integral model for turbulent buoyant jets in unbounded stratified flows. Part 2: Plane jet dynamics resulting from multiport diffuser jets. *Environmental Fluid Mechanics, 6*, 43–100.

Jirka, G. H. (2008). Improved discharge configuration for brine effluents from desalination plants. *Journal of Hydraulic Engineering, 134*, 116–120.

Kikkert, G. A., Davidson, M. J., & Nokes, R. I. (2007). Inclined negatively buoyant discharges. *Journal of Hydraulic Engineering Division of the American Society of Civil Engineers, 133*, 545–554.

Lindberg, W.R. (1994). Experiments on negatively buoyant jets, with and without cross-flow. In P.A. Davies & M.J. Valente Neves (Eds.), *Recent research advances in the fluid mechanics of turbulent jets and plumes, NATO, series E: Applied sciences* (vol. 255, pp. 131–145). Kluwer Academic Publishers

Matsuda, T., & Sakakibara, J. (2005). In the vortical structure in a round jet. *Physics of Fluids, 17*, 1–11.

Pantzlaff, L., & Lueptow, R.M. (1999). Transient positively and negatively buoyant turbulent round jets. *Experimental in Fluids, 27*, 117–125.

Papakonstantis, I. G., Christodoulou, G. C., & Papanicolaou, P. N. (2011). Inclined negatively buoyant jets 1: Geometrical characteristics. *Journal of Hydraulic Research, 49*, 3–12.

Papanicolaou, P.N., & Kokkalis, T.J. (2008). Vertical buoyancy preserving and non-preserving fountains, in a homogeneous calm ambient. *International Journal of Heat and Mass Transfer, 51*, 4109–4120

Pincince, A. B., & List, E. J. (1973). Disposal of brine into an estuary. *Journal of Water Pollution Control Federation, 45*, 2335–2344.

Roberts, P. J. W., Ferrier, A., & Daviero, G. (1997). Mixing in inclined dense jets. *Journal of Hydraulic Engineering Division of the American Society of Civil Engineers, 123*, 693–699.

Roberts, P. J. W., & Toms, G. (1987). Inclined dense jets inflowing current. *Journal of Hydraulic Engineering, ASCE, 113*(3), 323–341.

Shao, D., & Law W.-K. A. (2010). Mixing and boundary interactions of 30° and 45° inclined dense jets. *Environmental Fluid Mechanics, 10*(5), 521–553.

Simpson, J. E. (1987). *Density Currents: In the environment and the laboratory*. Chichester, U.K.: Ellis Horwood Ltd.

Suresh, P. R., Srinivasan, K., Sundararajan, T., & Sarit, D. K. (2008). Reynolds number dependence of plane jet development in the transitional regime. *Physics of Fluids, 20*, 1–12.

Tsihrintzisand, V.A., & Alavian, V. (1986). Mathematical modeling of boundary attached gravity plumes. In *Proceedings International Symposium on Buoyant Flows* (pp. 289–300), Athens, Greece.

Turner, J. S. (1966). Jets and plumes with negative or reversing buoyancy. *Journal of Fluid Mechanics, 26*(1966), 779–792.

Zeitoun, M. A., Reid, R. O., McHilhenny, W. F., & Mitchell, T. M. (1972). *Model studies of outfall systems for desalination plants*. Research and Development Progress Report No. 804, Office of Saline Water, U.S. Department of the Interior, Washington, DC, USA.

Zeitoun, M. A., McHilhenny, W. F., & Reid, R. O. (1970). *Conceptual designs of outfall systems for desalination plants*. Research and Development Progress Report No. 550, Office of Saline Water, U.S. Department of the Interior, Washington, DC, USA.

Zhang, H., & Baddour, R.E. (1998). Maximum penetration of vertical round dense jets at small and large Froude numbers, Technical Note No. 12147. *Journal of Hydraulic Engineering, ASCE 124*(5), 550–553.